

Evaluation of the impact of active wake control techniques on fatigue, ultimate loads and rotor design for a 10 MW wind turbine.

Alessandro Croce¹, Stefano Cacciola¹, Luca Sartori¹, and Paride De Fidelibus¹

¹Department of Aerospace Science and Technology, Politecnico di Milano, Milano, Italy

Correspondence: Alessandro Croce (alessandro.croce@polimi.it)

Abstract. Wind farm control is one of the solutions recently proposed to increase the overall energy production of a wind power plant.

A generic wind farm control is typically synthesized so as to optimize the energy production of the entire wind farm by reducing the detrimental effects due to wake-turbine interactions. As a matter of fact, the performance of a farm control is typically measured by looking mainly at the increase of the power production, properly weighted with the wind Weibull and rose at a specific place, and, sometimes, by looking also at the fatigue loads. However, an aspect which is rather overlooked is the evaluation of the impact that a farm control law has on the individual wind turbine in term of maximum loads and dynamic response under extreme conditions.

In this work, two promising wind farm controls, based respectively on Wake Redirection (WR) and Dynamic Induction Control (DIC) strategy, are evaluated at a single wind turbine level. To do so, a two-pronged analysis is performed. Firstly, the control techniques are evaluated in terms of the related impact on some specific key performance indicators (e.g. fatigue and ultimate loads, actuator duty cycle and annual energy production). Secondly, an optimal blade redesign process, which takes into account the presence of the wind farm control, is performed with the goal of quantifying the possible modification in the structure of the blade and hence of assessing the impact of the farm control on the Cost of Energy model.

1 Introduction and motivation

So far, the majority of the works devoted to wind farm control is aimed at evaluating the effectiveness of such techniques as means of power harvesting maximization. Among all, one can mention the methodologies based on wake steering (see Fleming et al. (2019); Gebraad et al. (2017, 2016)), steady axial induction (see Annoni et al. (2016)) and dynamic induction control, also called active wake mixing (see Munters and Meyers (2018, 2017)). When it comes to farm control synthesis, the energy production is typically viewed as the most significant merit figure, and seldom the fatigue loads on single wind turbine (WT) are considered within the control optimization problem (Bossanyi, 2018; Knudsen et al., 2015).

On the other hand, the quantification of the impact of wind farm control setpoint on turbine fatigue has been object of an extensive research in recent years, especially in relation to yawed operations (Cardaun et al., 2019; Ennis et al., 2018; White et al., 2018). All works suggested that the impact of misalignment depends strongly on ambient conditions (vertical shear and turbulence intensity).

Boorsma (2012) evaluated the fatigue loads of a 2.5 MW turbine operating in misaligned conditions using different aerodynamic models, and compared the results with field measurements. **It was shown that the combination of vertical shear layer and misalignment may lead to increase or decrease of fatigue loads, depending on the sign of the yaw misalignment angle.**

30 A similar study **with similar conclusions**, based on a dedicated and systematic test campaign on the field, is presented in Damiani et al. (2018), for a 1.5 MW turbine.

Zalkind and Pao (2016) analyzed the impact of wake redirection control in terms of fatigue loads considering a simple two-turbine cluster and a reference wind rose. **The aggregate damage equivalent loads was computed from the actual yaw misalignment angles which the upstream turbine would experience for maximizing the total power of the cluster. In such an ideal case, the impact of wake redirection control resulted to be small due to the amount of time spent with no yaw misalignment.**

35 Mendez Reyes et al. (2019) and Kanev et al. (2018) considered the problem of quantifying the fatigue loads of downstream turbines impinged by the wakes shed by upstream machines. Both studies concluded that impinging wakes are typically more detrimental in terms of loading than operating with yaw misalignment, and hence, that wake redirection is expected to reduce the overall lifetime fatigue thanks to the mitigation of rotor-wake interactions.

40 Finally, Frederik et al. (2020b) provided the first evaluation of the impact on fatigue of dynamic induction control, considering a reference 5 MW turbine model.

Despite the availability of such relevant results, the question over the actual impact of farm control on rotor design is still open, primarily because the fatigue is seldom evaluated in all those conditions prescribed by the Standards for design and certification of wind turbines. Moreover, according to the farm control logic, a turbine may experience significant increases not only in the fatigue, but also in the ultimate loads or maximum blade deflections, which typically come from extreme events, as gusts and/or faults, and may represent critical design drivers.

Fatigue, ultimate loads and maximum tip displacements participate together in the definitions of the constraints to which a machine is subject during the design phase. Hence, the possible increase in machine loading induced by wind farm control determines whether a turbine structure is to be re-designed, with an eventual increase of its mass and cost, or not.

50 This consideration is of paramount importance as the turbine design and the resulting CoE can be considered as the ultimate indicators of the effectiveness of a farm control strategy.

As expected the advantages (i.e. the increased power production at farm level) and the disadvantages (i.e. the possible increased loading at turbine level) of a farm control have to be combined to determine their impact in terms of cost of energy (CoE). In order to show this concept, one may consider the simple definition of the CoE of a single turbine, reported in Fingersh et al. (2006),

55
$$\text{CoE} = \frac{\text{FCR} \cdot \text{ICC}}{\text{AEP}} + \text{AOE},$$

where FCR is the fixed charge rate, ICC the initial capital cost, consisting mainly in the turbine cost, and AOE the annual operating expenses (expressed **per** unit energy yield), which may include land or sea lease and operation and maintenance costs. Clearly, the AEP of a single turbine may be reduced or increased by the farm control according to the fact that a

machine operates mainly upstream or downstream. The sum of the AEPs of all turbines belonging to the farm increases for
60 a farm control neatly designed. Besides that, the related effect on the turbine loading and, eventually, on ICC, is still to be
carefully determined in order to find the final effect on CoE.

To do so, given a specific wind farm control **technique**, the component loading should be evaluated on a turbine level, so as
to clarify if a generic turbine within a “controlled farm” would need a dedicated design and, consequently, evaluate the effect
of the farm control in terms of ICC.

65 The scope of this paper is twofold. First, to quantify the impact of two wind farm control **strategies**, i.e. wake steering and
dynamic induction control, at turbine level through some indicators strictly connected to machine design, which are fatigue
and ultimate loads and maximum blade tip deflection, computed according to the present Standards. **To the best of the Au-**
thors’ knowledge, the implications of farm control in terms of ultimate loads and maximum blade deflection have never been
addressed, hence this part of the work represents the major source of novelty of the paper. Second, in order to provide an
70 insight in the impact of farm control on the cost of the rotor, an optimal blade re-design process is performed, which takes into
consideration the most critical wind farm control law.

As the design of a new rotor has to be carried out according to the Standards and has to consider the worst possible scenario,
the analyses in this paper will focus on the isolated upstream machine, under different farm-related operating conditions. In
fact, as it will be pointed out in detail in Sec. 2, in the simple case of wake redirection control, upstream turbines are more
75 **prone to the negative impacts of the farm control, e.g. those entailed by operations at large yaw angles, while the downstream**
ones will possibly experience all the advantages, e.g. lower turbulence and lower wake impingement with respect to the case
without wind farm controllers.

Clearly, in a single farm, there is a subset of machines which see most of the time a clean flow, i.e. the outermost ones
exposed according to the most probable wind direction, and another subset of turbines, the innermost ones, which sometimes
80 see a waked flow. In this scenario, it is certainly interesting to evaluate a possible usage of partially customized or totally
different turbines in a single farm, depending on the specific machine location. In such a case, the turbines proposed for the
innermost farm locations may be characterized by more competitive designs thanks to the farm control. Although extremely
interesting, this idea falls out of the scope of the present paper.

In this work, all analyses are performed on the INNWIND.EU 10 MW wind turbine (DTU, 2012), which can be considered
85 as a generic reference model for future machines proposed for the exploitation of on- and off-shore resources.

The present paper is organized as follows. Sections 2 and 3 deal with the explanation of the methodologies adopted to
evaluate the impact of wind farm control on single wind turbine level. These sections include the description of the wind
turbine used for the present analysis and its controller, of the multibody software used for the aeroservoelastic simulations
and of the optimal rotor design tool. In Sec. 4, a sensitivity analysis on the effects of two wind farm control techniques (i.e.
90 WR and DIC) is considered. Specifically, fatigue and ultimate loads, along with maximum blade tip deflection, are evaluated
considering different setting of the control techniques (e.g. different yaw misalignment angles for wake redirection technique)
in order to find the most impacting conditions for the turbine. Such sensitivity analysis is viewed as a preliminary step for the

optimal blade design process which is described in Sec. 5. Finally, Sec. 6 concludes with a listing of the main findings and possible outlooks of the work.

95 2 Methodology

Having an overview of the effects that a **wind farm control** has on the single wind turbine and eventually quantifying its impact on the design of the rotor is not an easy task. In fact, when dealing with **an entire wind farm**, the problem of analyzing wind turbine performance becomes highly site specific because the inputs of the **farm control** will depend on many factors, such as the farm layout, the wind distribution and rose, the turbulence intensities. In such a scenario, deriving conclusions of general
100 validity without focusing too much on a specific case is a difficult task.

Moreover, in the same wind farm, a turbine may act according to a farm control input (e.g. operates at a specific yaw misalignment angle to redirect its wake) and/o feel the effects of the control action performed by another machine, depending on whether it is up- or down-stream with respect to the wind direction. As a consequence, one should have to model all possible cases to have a global overview. This clearly poses some difficulties as the study would result to be again strongly dependent
105 on the **farm** geometry and would lose, at least in part, its generality.

Last but not least, modern wind turbines are designed according to international Standards, which prescribe the computation of fatigue and ultimate loads in a certain number of conditions, e.g. for specific wind speeds and turbulence intensity levels. Hence, the impact of a farm control should be evaluated through those Standards specifications. Although adhering to Standards poses some limitations to the analyses, e.g. fatigue is verified only for a single shear layer exponent and for specific
110 combinations of wind speed and turbulence intensity, it is only through such an approach that one can evaluate the “practical” impact of wind farm control on turbine design. Unfortunately, regulations, in their current status, do not consider yet the fact that a turbine may operate out of the design conditions according to a farm control.

This discussion highlights the fact that there are three critical issues in this study which should be neatly addressed: site-dependency of the problem, if and how to consider the effects of wind farm control on downstream machines and inclusion of
115 the farm control within the Standards.

To overcome the first point, in this work, all analyses have been conducted as sensitivity studies, in which the effects of the **wind farm control** are considered as functions of some important wind farm control parameters. Hence, the study of the wake redirection was carried out for different values of yaw misalignment, whereas that of the DIC for different frequency and amplitude values of the pitch oscillation. From this point of view, such a sensitivity analysis can be even used as input for the
120 synthesis and fine tuning of a farm control by reducing its authority **in conditions which** could be critical from the loading **side**. **For example, since a turbine operating in yawed conditions is more exposed to extreme events (i.e. gusts, or extreme shear), it could be interesting to bound the operational range of the controller within certain values of misalignment, in order to limit the increase of the driving loads.**

Otherwise, the amplitude and the frequency of the pitch motion for dynamic induction control can be chosen also by looking
125 at the effect of fatigue and actuator duty cycle. This possibility, although interesting, is not considered in this paper, as it is out
of its scope, and will be further investigated as a follow-up of this work.

Dealing with the effects of the farm control on downstream machines, it is important to stress the fact that real turbines
typically operate in a farm and are certainly **influenced by** wake interaction phenomena. **Despite that, when a wind farm comes
to its end of service, most turbines still have some residual life to exploit** (Ziegler et al., 2018). For this reason, even if wake
130 interactions represent a significant source of loading, as demonstrated in some recent publications (Mendez Reyes et al., 2019;
Kanev et al., 2018), one could conclude that modern design procedures and regulations are adequate to guarantee safe wind
turbine operations even in presence of normal wake impingement events. Accordingly, the analyses conducted in this work
refer only to the upstream turbine, i.e. the one which performs an action according to the control of the farm; an aspect which
is actually not considered in current design procedures.

135 The discussion about the Standards deserves a special attention. To this end, consider a simplified wind farm made by three
INNWIND.EU 10 MW turbines. Figure 1, left **panel**, represents a simulated flow within such a **farm** on a plane parallel to the
ground at hub height. The flow has been simulated with the open-source version of Floris (FLOW Redirection and Induction
in Steady State) written in Python (see NREL (2019)). The wind, 8 m/s with turbulence intensity of 2%, is coming 35 deg
North-West and, as visible from the upper plot, generates strong wake impingement between the first and the second turbine,
140 and between the second and the third. In this situation it is possible to increase the power harvested by the farm by yawing
the turbines so as to redirect their wakes as demonstrated by the bottom plot. The yaw misalignment angles of the first two
turbines have been computed in order to maximise, throughout the optimal yaw angle setpoints, the total power production. In
this case, within the limits of this stationary model, these angles are about -20 and 24 deg, respectively. The very same analysis
and optimization have been carried out for different wind speeds and different turbulence intensity levels. Figure 1, on the
145 right, shows the contour plot of the optimal yaw angle of the first turbine. Clearly, for low speed and low turbulence intensity
the turbine has to **yaw significant yaw angles** (higher than 20 deg) to optimize the energy production. On the other hand, as
the wind speed increases, the optimal yaw decreases up to zero in the full power region, where the farm control is no longer
needed. Additionally, since higher turbulence levels are responsible for an increased in-wake flow mixing and in turn faster
wake dissipation, the yaw angle decreases also as TI increases. The dark blue line refers to a yaw angle of 2 deg and, hence, can
150 be viewed also as the boundary between the two regions where the farm control is active or not. Superimposed to this contour,
the plot displays also the conditions prescribed by the Standards IEC-6400 for the computation of the Design Load Cases
(DLCs) for turbine class IA (IEC 61400-1 Ed.3., 2004), as black lines and triangles. Just at a first sight, one may recognize that
the majority of the conditions considered in the Standards **seem** out of the region of activation of the control, especially those
at Extreme Turbulence Model (ETM) and Nominal Turbulence Model (NTM), the latter used for fatigue calculation. Extreme
155 Wind Shear (EWS), Extreme Change of Direction (ECD) and Extreme Operating Gust (EOG), on the other side, refer to steady
winds and are associated to an ideal null TI. In this situation, the analysis appears extremely complicated, especially because of
the dependency of the optimal yaw angle on the TI, which, **given** the current state of the regulation, would practically exclude
the farm control from NTM and hence from fatigue and AEP calculation. Moreover, a further question arises over the actual

implementation of the control, on whether it can rely on a good measure of TI and is synthesized so as to account for it. This stresses two facts. First, including a TI-dependency of the control in this analysis is problematic and second, an update of the Standards to consider wind farm control is in any case necessary. The latter issue, although important and interesting is out of the scope of the paper. Dealing with the TI-dependency, in order to provide an analysis of general validity and to simplify the treatment, the work of this paper considered only a wind speed-dependency of the control and imposed as limit for its activation 15 m/s no matter of TI. Clearly, these assumptions appear strong, but they allow one to focus directly on the worst scenario and hence to show the maximum possible impact of the wind farm control on turbine loading. In fact, from the design standpoint, one is more interested in the worst case rather than in a specific one (i.e. a specific farm layout, wind rose and control implementation), because a machine is designed to safely operate in different sites, farms and locations within a single farm.

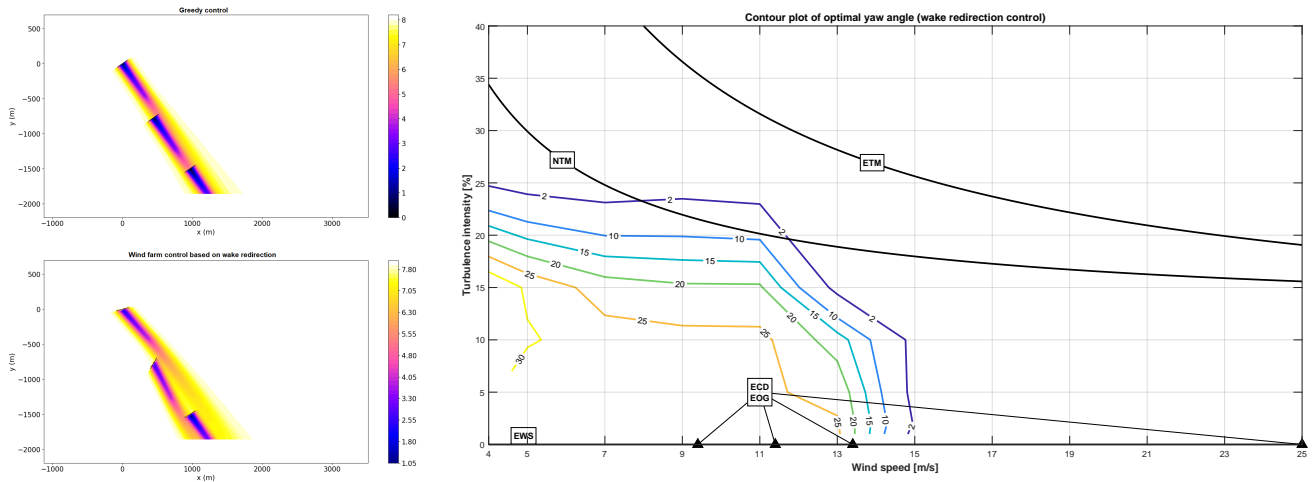


Figure 1. Investigation of wake redirection technique as function of wind speed and TI. Left plot, Floris simulation of three-turbine farm at 8 m/s and TI 2%. Right plot: contour of optimal yaw angles of the first turbine superimposed to the conditions prescribed by Standards for design load cases (DLCs) calculation.

3 Analysis and design framework

In this work we use the INNWIND.EU 10 MW wind turbine (DTU, 2012) as a reference for all parametric analyses and design activities. All dynamic simulations are run by our in-house multibody solver C_p - Λ (Bottasso and Croce, 2009–2018; Bottasso et al., 2006). This tool allows to model the flexibility of blades, tower and shafts through 1D geometrically exact beam model (Bauchau, 2011) coupled to full 6×6 mass and stiffness matrices. Aerodynamics is rendered via the classical BEM theory with hub- and tip-losses and tower shadow. First and second order dynamical models are employed to include respectively generator and pitch actuator dynamics.

The control of the turbine in operating conditions is managed by the CL-WINDCON standard controller (CL-Windcon, 2016-2019; IK4 Research Alliance, 2016), while non-operating conditions like faults, startups, shutdowns and parking are all managed by the *POLI-Wind Supervisor* (Riboldi, 2012), that also supervises the transitions between different operating states to ensure a smooth variation of the control variables.

180 The design and optimization activities are run by $C_p\text{-Max}$, a tool for the integrated design of wind turbines jointly developed by Politecnico di Milano and the Technische Universität München. A detailed description of the algorithm is provided by Sartori (2019) and by Bortolotti et al. (2016), together with a range of design applications focusing on the development of next-generation wind turbines.

Thanks to its multi-level architecture, $C_p\text{-Max}$ is able to both optimize the general features of the turbine (rotor diameter, tower height, tilt and cone angle) and to conduct specific optimization of the turbine subcomponents like blades, tower and generator. 185 This double capability is achieved through the coupling of a Macro Design Loop (MDL) and several design submodules. In this work, we only use the Structural Design Submodule (SDS), whose workflow is shown in Fig. 2.

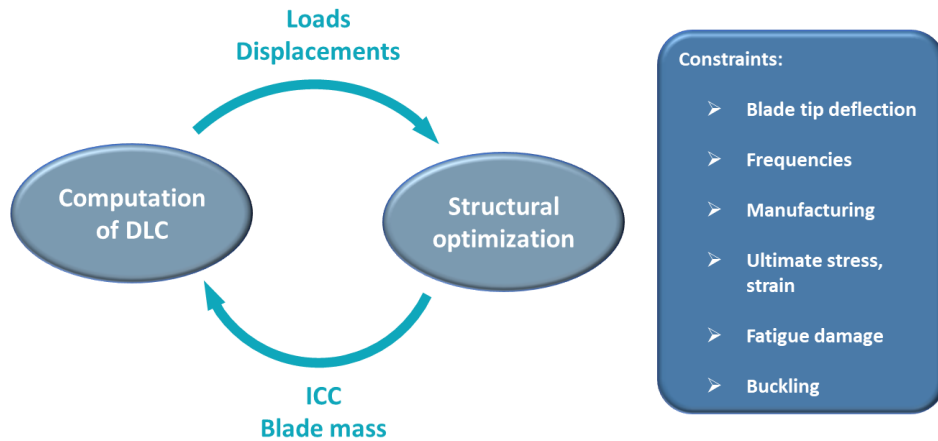


Figure 2. Architecture of the Structural Design Submodule (SDS).

The purpose of the SDS is to manage the structural design of the rotor through a dedicated optimization in which the thicknesses of all structural components are optimized to minimize the turbine ICC. As shown in the Figure, the structural optimization is conducted through a multi-steps procedure: initially, an arbitrarily large set of Design Load Cases (DLCs) is computed with $C_p\text{-Lambda}$ to extract the driving loads and displacements from fully-resolved aeroelastic simulations. 190 Once loads and displacements are computed, the structural optimization begins and the internal thicknesses are modified until a convergence solution is found. Then, if the optimal blade mass is different from the initial, the whole process (DLC + structural design) is repeated, so that the design can always account for the updated load spectra. Along this process, structural integrity constraints are enforced according to international certification guidelines. Those account for maximum deflections, 195 stiffness, strength, possible manufacturing limitations, fatigue and buckling.

Given the complexity of the problem at hand, any design-oriented activity should be planned out carefully as to identify the best trade-off between modelling accuracy, computational effort and design scope. In this view, we introduced some design assumptions in order to find a good balance between scope and CPU time. Our first choice was to limit the redesign effort to the optimization of the blade structure. In fact, although wind farm controllers may impact other aspects of the design, it is reasonable to expect that they significantly affect the driving loads, with important implications on the rotor structure. As a consequence, the macro parameters of the wind turbine like the rotor radius and tower height have not been modified through this activity. Similarly, the aerodynamic shape of the rotor has been kept constant and coherent to that of the baseline. It must be noticed that, by introducing this scope limitation, it was possible to include a large set of fully-resolved DLCs directly in the design, without the need to adopt any simplification on the load spectra. In particular, it was possible to use the set of DLCs listed in Table 1, defined according to the chosen standards IEC 61400-1 Ed.3. (2004). The entire set includes about 130 load cases, for a total computational time of 26~28 hours on a common desktop.

Table 1. Definition of the DLCs considered in the analyses.

DLC	Wind Type	Wind speed	Horizontal Misalignment	Fault	Safety Factor	Performance indicator
1.1	NTM	$V_{in} : V_{out}$	-	-	1.0	AEP, ADC, Fatigue
1.2	NTM	$V_{in} : V_{out}$	-	-	1.35	Ultimate
1.3	ETM	$V_{in} : V_{out}$	-	-	1.35	Ultimate
1.4	ECD	$V_r, V_r \pm 2, V_{out}$	-	-	1.35	Ultimate
1.5	EWS	$V_r, V_r \pm 2, V_{out}$	-	-	1.35	Ultimate
2.1	NTM	$V_{in} : V_{out}$	-	Grid Loss	1.35	Ultimate
2.2 PF	NTM	$V_{in} : V_{out}$	-	Pitch Freeze	1.35	Ultimate
2.2 PR	NTM	$V_{in} : V_{out}$	-	Pitch Runaway	1.35	Ultimate
2.3	EOG	V_r, V_{out}	-	Grid Loss	1.1	Ultimate
6.1	EWM	V_{ref}	-8 : 8 deg	-	1.35	Ultimate
6.2	EWM	V_{ref}	-180 : 180 deg	Grid Loss	1.1	Ultimate
6.3	EWM	V_{ref}	-20 : 20 deg	-	1.1	Ultimate

4 Sensitivity analysis about the effects of wind farm control on turbine level

The Standards require a turbine to be designed under a full list of design loads cases which include normal operative conditions, as well as situations where the machine undergoes extreme events or faults, and also cases in which the turbine is parked. Clearly, according to the specific case, we can either reasonably consider or completely exclude that the turbine may operate in a wind-farm-controlled regime.

For example, it may happen that, for a specific turbine and for a specific sub-component, the related ultimate load, noted U^* , comes from a case in which the wind farm control is not active (as for the DLC in parked conditions). In this case, it is possible

215 and foreseeable that the wind farm control **may entail** a general increase of machine loading, but if such increase is not enough to exceed U^* , the wind farm control has not any effect on that load.

Along with the list of DLCs, it is necessary to select the range in which the wind farm control is active. Clearly, the activation of the wind farm control is based on the specific implementation of the control scheme, and may depend on wind speed, turbulence intensity, geometry of the farm and even on combinations of the previous factors. In this very complex scenario, 220 in order to simplify the analysis and make it of general validity, the farm control is considered active only in a range of wind speeds (i.e. up to a given speed), no matter of the turbulence intensity or other factors.

4.1 Evaluation of the impact of wake redirection technique

In this Section the effects of the wake redirection control on fatigue and ultimate loads are investigated.

The wind farm control based on the wake redirection technique consists in yawing an upstream turbine by a specific amount 225 in order to deflect its wake out of one or more downstream turbines. Within such a wind farm control scenario, while the upstream machine experiences a loss of power, due to the wind misalignment, the downstream ones produce more power thanks to a reduced wake impingement.

In this work, the turbine misalignment is reproduced in the simulations by rotating the nacelle. Positive angles are associated to counterclockwise rotations of the nacelle viewed from above. Hence, the turbine experiences positive yaw misalignment 230 when the wind is coming from the right side, for an observer sitting on the hub and looking at the wind. In the reference configuration (i.e. for a null yaw angle) the wind is assumed to blow from North to South and, accordingly, the nacelle is oriented towards North.

In order to have an investigation of general validity, without being limited to a specific turbine and a specific wind farm, a sensitivity analysis has been carried out. In particular, the effects of different steady yaw misalignment between -30 and 30 235 degrees on turbine fatigue and ultimate loads have been evaluated.

The 10 MW INNWIND.EU model, implemented through the software C_p - Λ , was subjected to the full list of DLCs described in Tab. 1. As already explained in Sec. 1, DLC 6.x series was simulated only for the reference turbine (i.e. without misalignment), whereas DLC 1.x and 2.x for reference and for other four different yaw misalignment angles (± 15 , ± 30 deg).

The plot on the left of Fig. 3 shows the blade root flapwise DEL increment associated to the wake redirection for different 240 yaw angles. These DEL loads have been computed in power production with turbulent wind from the cut-in to the cut-out wind speed (DLC1.2) and then weighted with the Weibull probability function for a class IA (IEC 61400-1 Ed.3., 2004). In this analysis, and in the following ones, an equivalent frequency corresponding to 10M cycles in 20years has been considered. Moreover, the following inverse SN-curve slope (i.e. **Wöhler exponent**) values have been considered: $m = 10$ for the composite blades and $m = 3$ for the steel tower. It's important to stress here that only for wind speed lower than 15 m/s the wind farm 245 controller (i.e. the wake steering) is active, so that at higher wind speeds there is no difference between the baseline and the wind-farm-controlled ones. **As a side remark, limit the activity of the farm control to 15 m/s is reasonable for controllers aimed at maximizing the power production. It is however possible to have a farm control activity also beyond this wind speed for downstream fatigue mitigation, as proposed in Urbán et al. (2018).** The same figure hence shows that the overall

effect of the yaw misalignment on the cumulated DEL is limited, with an increase of slightly more than 3% at -15 deg. The
 250 reduction experienced in most of the positive misalignment range is due to the coupling between vertical shear layer and
 lateral flow velocity induced by yaw misalignment. In fact, vertical shear layer increases the blade loads when it is upward
 and decreases them when downward, generating a load oscillation at the rotor frequency. A lateral component of the wind
 is similarly responsible for oscillating loads, but with the difference that the increment may occur when the blade is upward
 or downward depending on whether the misalignment angle is positive or negative. As a consequence, the impact of yaw
 265 misalignment may be summed up to or subtracted from the one of the shear layer. This fact was also noticed in (Boorsma,
 2012; Ennis et al., 2018).

The assessment of the impact of fatigue on the tower requires special attention. Since the tower orientation remains fixed
 regardless of the yaw angles, a separate analysis for fore-aft and side-side directions lacks of generality. In fact, one may expect
 the yaw angle to differently impact on the moments computed about two orthogonal directions like, for instance, fore-aft and
 260 side-side. As a consequence, the analysis must consider fatigue loads coming from the worst possible direction and, to do so,
 it is possible to proceed as follows.

Let define $\rho \in [0, \pi]$ a generic angle computed with respect to North and positive counterclockwise. Then, $M_\rho(t; \rho)$ is the
 time-varying physical moment about a direction which is rotated by an angle ρ . From the time history of $M_\rho(t; \rho)$ it is possible
 to compute the *directional* DEL indicated with $M_{\rho_{\text{DEL}}}(\rho)$ and to identify its highest value, $M_{\rho_{\text{DEL}}}^{\text{max}} = \max(M_{\rho_{\text{DEL}}}(\rho))$ and
 265 the associated *worst direction* $\rho_{\text{max}_{\text{DEL}}} = \arg(\max(M_{\rho_{\text{DEL}}}(\rho)))$.

The plot on the left of Fig. 4 gives an example of the directional DEL $M_{\rho_{\text{DEL}}}$ computed at tower base for three different yaw
 angles. The distributions of directional DEL has been obtained by collecting output from different load sensors at the tower
 base (rotated every 15 degrees) and then interpolated. For each distribution, a diamond marker identifies the maximum load
 $M_{\rho_{\text{DEL}}}^{\text{max}}$ and the corresponding worst direction $\rho_{\text{max}_{\text{DEL}}}$. It can be seen that for a zero yaw (solid blue line) the worst direction
 270 lies close to 90 degrees which, in the considered configuration, corresponds to both a North/South and the fore-aft bending
 moments. Once the rotor is rotated (dashed and dotted lines), the two directions are no longer aligned and the worst direction
 occurs at different angles ρ depending on the yaw angle, as shown in the right plot of Fig. 4.

The plot on the right of Fig. 3 shows the increment in the maximum directional DEL $M_{\rho_{\text{DEL}}}^{\text{max}}$ for tower base as function of
 the yaw angle. Again, operating in yawed condition (for wind speed below 15m/s) does not seem critical in terms of fatigue
 275 for the tower base.

Figure 5 shows the ultimate load increment associated to the wake redirection for different yaw angles for blade root com-
 bined moment (left) and tower base combined moment (right). The text above each bar indicates the DLC which has generated
 such maximum loads. In terms of blade, the effect of yaw misalignment is limited with just a small increase of about 1% at 30
 deg. Loading on tower seems to suffer a bit more at high misalignment with an increase of 7.5% at 30 deg.

280 The analysis of blade tip displacement, on the other hand, shows an increase of tip displacement up to 6% as shown in
 Fig. 6. This increment, although apparently small, deserves a special attention. In fact, often, the blade design is constrained
 by the maximum tip deflection which is to be bounded in order to avoid dramatic blade-tower collision. Since the maximum

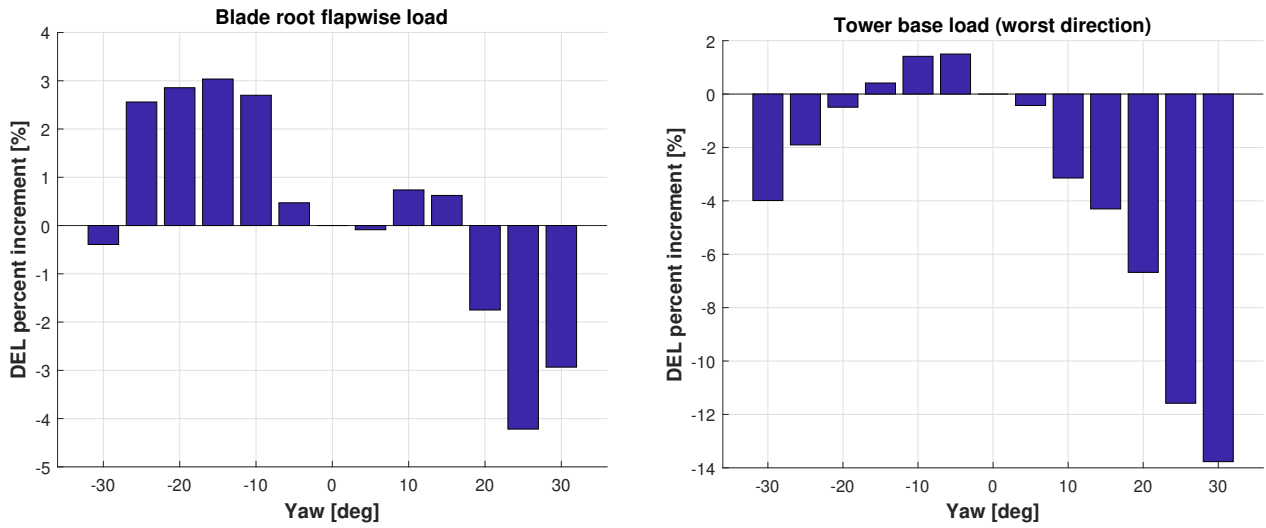


Figure 3. Comparison of blade root flapwise DEL (left) and tower base maximum directional DEL, $M_{\rho_{DEL}}^{\max}$ (right).

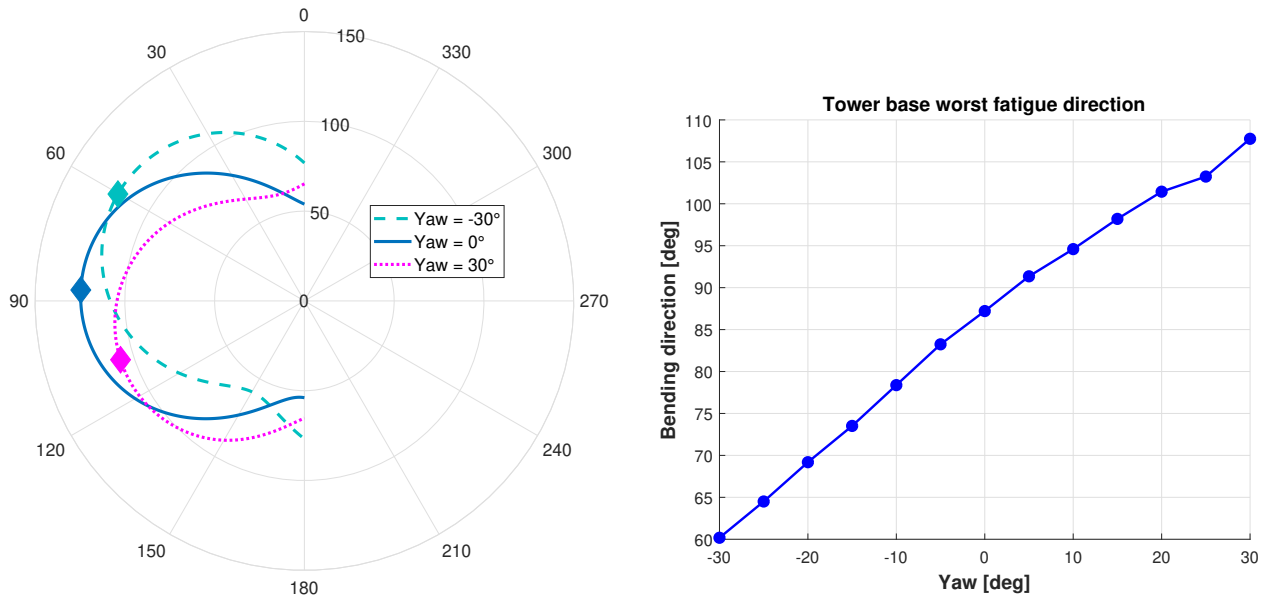


Figure 4. Directional fatigue at tower base. Left plot: directional DEL [MNm] at tower base for three yaw angles; diamond markers identify the maximum value. Right plot: worst fatigue direction at tower base as a function of yaw angle.

tip deflection typically enters in the design process as a constraint, it is possible that even a small increment of this value may lead to a violation of this constrain and in turn to the need of a blade redesign.

285 By looking at these results, one may also conclude that avoiding operating at very high misalignment (i.e. at 30 deg) may be beneficial. In fact, up to ± 15 deg, the increment of both fatigue and ultimate loads, seem essentially limited. It is important

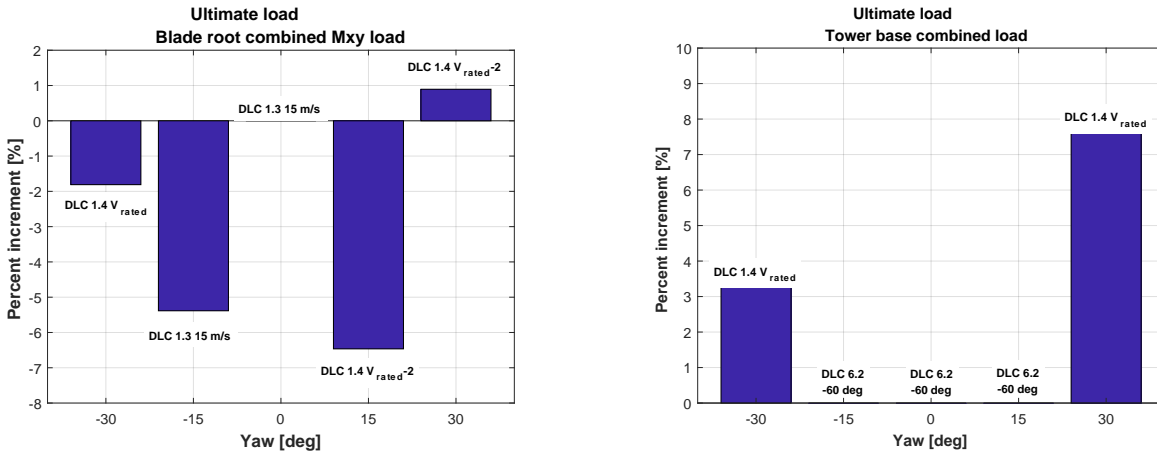


Figure 5. Comparison of ultimate loads. Left: blade root combined moment. Right: tower base combined moment.

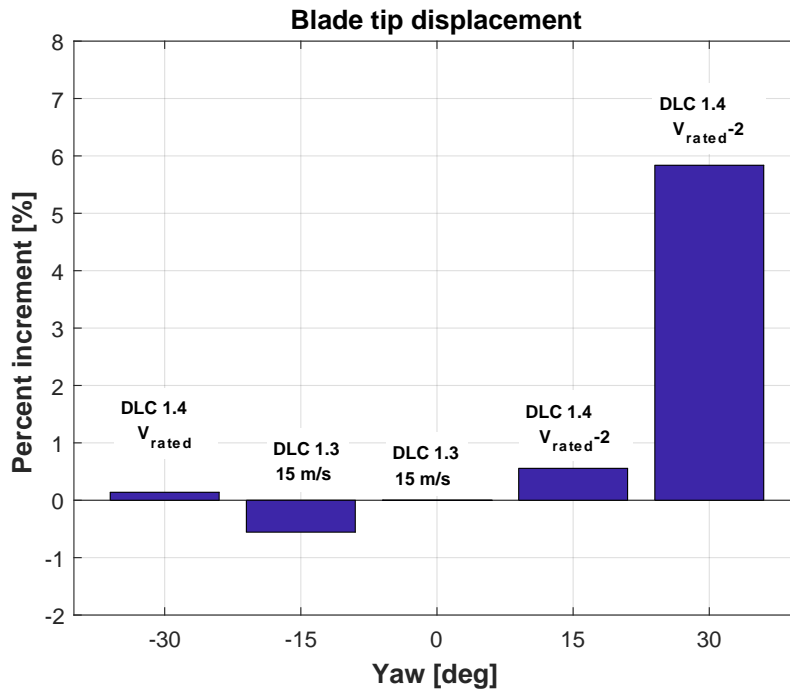


Figure 6. Comparison of maximum blade tip displacement.

to stress that the sensitivity analysis shown in this section allows the designer to estimate the extreme parameters of this wind farm control technology to be applied to already existing wind farms. These limits are defined by the design loads of the single wind turbine: the wind farm operators may apply this farm controller as far as the loads induced by this technology do not overtake the design ones.

In terms of actuator duty cycle, the wake redirection does not seem problematic. In fact, when a turbine operates in yawed condition, it experience lower winds. This makes the turbine work in below-rated region, with limited pitch activity, for a higher amount of time. A quantitative evaluation shows a decrease of 41% in ADC for a misalignment of 30 deg.

Finally, AEP results to be highly affected as single machine may experience a loss up 18% at -30 deg. This result is already
 295 known to the scientific community and is generally balanced by the increase in power of the downwind wind turbine(s).

4.2 Evaluation of the impact of dynamic induction control

4.2.1 Review of dynamic induction control

Another interesting means of increasing the total wind farm power consists in the so-called Dynamic Induction Control (DIC). Specifically, the upstream wind turbine, when its wake impinges on a downstream machine, modulates the thrust in a periodic
 300 way. The modulation can be performed by pitching collectively or cyclically the blades at a specific frequency or by changing the rotor speed. Clearly, the most effective action is to enforce a Periodic Collective Motion (PCM) of the blade pitch angles. The effect of the PCM is to dynamically vary the induction of the rotor and, hence, to increase the mixing level inside the wake. The wake itself results to be energized by such fluctuating induction and recovers in a faster way. This technique was recently studied through CFD simulations (Munters and Meyers, 2017, 2018) and validated in a scaled wind tunnel experimental
 305 campaign (Frederik et al. (2020b)).

The DIC technique studied here is a pure PCM at a single frequency, as described by

$$\beta_{\text{PCM}} = A_{\text{PCM}} \sin(2\pi f_{\text{PCM}} t + \varphi_{\text{PCM}}), \quad (1)$$

where β_{PCM} is the pitch setting imposed by PCM to be summed up to the pitch of the trimmer, A_{PCM} is the related amplitude, f_{PCM} the frequency, t the time and φ_{PCM} the possible phase.

310 **Despite** the limited number of studies devoted to PCM, especially if compared with the amount of literature available about wake redirection technique, it is already possible to highlight some important concepts:

- PCM seems effective in increasing the total wind farm power output by some percent, as demonstrated by both simulations and wind tunnel experimentation.
- The increase in wind farm power depends strongly on the amplitude and frequency of the rotor thrust variation.
- 315 – Rather than in terms of frequency f , the effect of the PCM technique is to be viewed in terms of the dimensionless Strouhal number S_t , defined as

$$S_t = \frac{f_{\text{PCM}} D}{U_\infty}, \quad (2)$$

being D the rotor diameter and U_∞ the undisturbed wind velocity.

320 – The optimal Strouhal number was found to be 0.25 in CFD simulation (see Munters and Meyers (2018)), whereas in wind tunnel it was possible to verify significant power increases in a wider range between 0.17 and 0.45 (see Frederik et al. (2020b)).

4.2.2 Effect of PCM amplitude and Strouhal number on turbine loading

Different combinations of amplitude β_{PCM} and Strouhal number S_t were considered: the range in amplitude was set between 1 and 4 deg, whereas the range of Strouhal between 0.2 and 0.5, according to the findings of an experimental campaign in wind tunnel (see Frederik et al. (2020b)).

At first, consider AEP, ADC and fatigue loads (DLC 1.1 and DLC 1.2), again under the assumption that PCM is active only below 15 m/s. The loss of AEP of the upstream wind turbine results very low. As example, the case of $\beta_{PCM} = 2$ deg and $S_t = 0.5$ is associate to a loss of AEP equal to 0.5%. On the other hand, considering a higher amplitude, $\beta_{PCM} = 4$, the decrease of AEP results 2.2%.

Dealing with the Actuator Duty Cycle (ADC), the effect of PCM is way more significant. In particular, considering $S_t = 0.5$, the increase of the ADC results equal to 77% and 143% respectively for $\beta_{PCM} = 2$ and $\beta_{PCM} = 4$.

Figure 7 shows DEL as a function of the wind speed for blade root flapwise moment (left) and tower base N-S moment (right), in the case of $\beta_{PCM} = 2$ and $S_t = 0.5$, as an excerpt from the results. The increase in DEL of the PCM (dashed line) with respect to the reference, i.e. without PCM, turbine (solid line) is pretty visible. Apparently, higher velocities are associated to more significant increases. This fact demonstrates that the maximum wind speed at which the wind farm control is active is to be carefully selected, in order to find a good balance between optimizing power output and increasing loads.

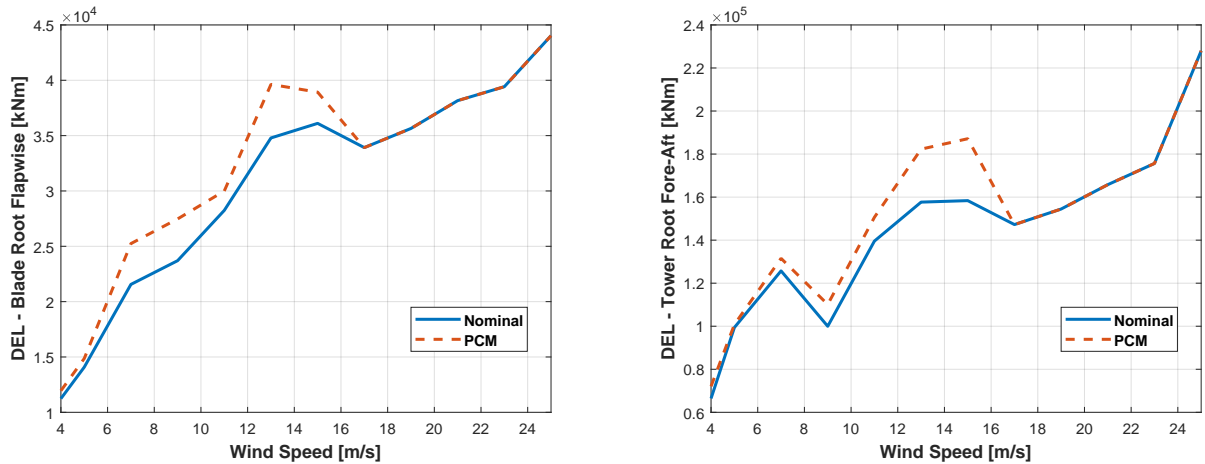


Figure 7. DEL comparison for different wind speed values and with $\beta_{PCM} = 2$ and $S_t = 0.5$. Left: blade root flapwise moment. Right: tower base F-A moment.

A sensitivity analysis was also performed so as to compute the effect of PCM in term of DEL as functions of Strouhal number and amplitude. Figure 8 shows the percentage DEL increment for different combination of Strouhal number and amplitude for blade root flapwise (left) and tower base (right). As expected, the highest increases are associated to larger pitch amplitudes and Strouhal numbers.

For both blade flapwise and tower base, the effects are significant and may amount to 20% and 30%, respectively, in the worst cases ($\beta_{PCM} = 4$ and $S_t = 0.5$). However, if one excludes the highest amplitude limiting the authority of PCM to 2 deg, the detrimental effect of PCM in terms of fatigue seems acceptable, being equal to about 10% for both loads.

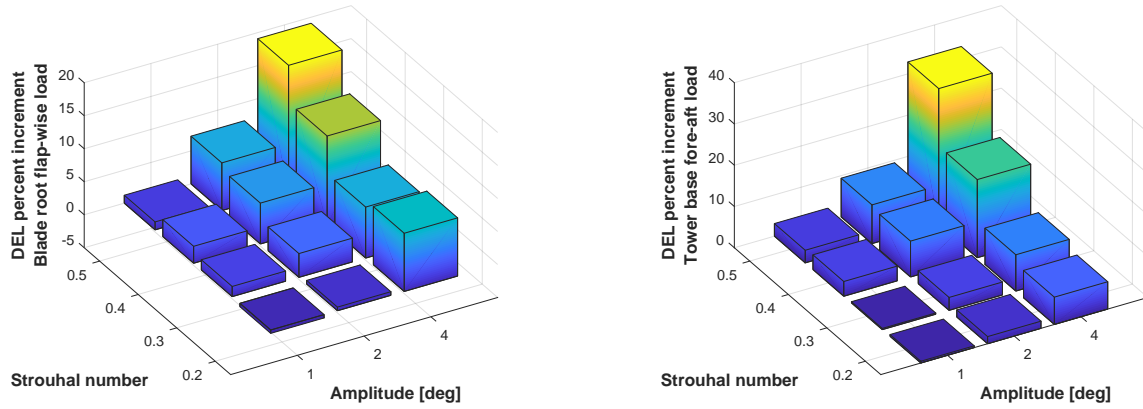


Figure 8. Weibull weighted DEL increases as function of amplitude and Strouhal number. Left: blade root flapwise moment. Right: tower base F-A moment.

The DEL on the blade root edgewise, not shown here for the sake of brevity, is mildly influenced (increase of about 1.5% in the worst case). This result is not surprising as the loading in edgewise direction is mostly governed by gravity rather than aerodynamics. Similar conclusions can be derived for the nodding and the yawing moments, depicted in Fig. 9, for which the effect of PCM is quantifiable in less than 1.5%.

Particular attention should be devoted to the impact of PCM on downstream rotor loading. **The change of thrust, in fact, results in a higher in-wake velocity, but also creates a low frequency flow travelling downwind.** The impact of such a pulsating flow with downstream machines can be significant in terms of turbine loads and aero-servo-elasticity. This particular study, out of the scope of the present paper, is currently under investigation, and preliminary results are available in Cacciola et al. (2020a).

A detailed analysis concerning the ultimate loads has been carried out as well. It was primarily observed that the phase of the oscillation φ_{PCM} is of paramount importance. Consider for example the set of DLCs including extreme conditions. By chance, it is possible that the particular extreme event, like a gust or a fault, occurs at a time in which the PCM control is increasing the collective pitch, thereby reducing the rotor loading. In this case, the peak of the load involved by the extreme event could be smoothed. Conversely, if the extreme event had occurred in correspondence of a decrease of the collective pitch, the effect of the control would have been that of increasing the load. This is due to the difference between the characteristic time of these extreme events (a few seconds) with respect to the PCM period (tens of seconds).

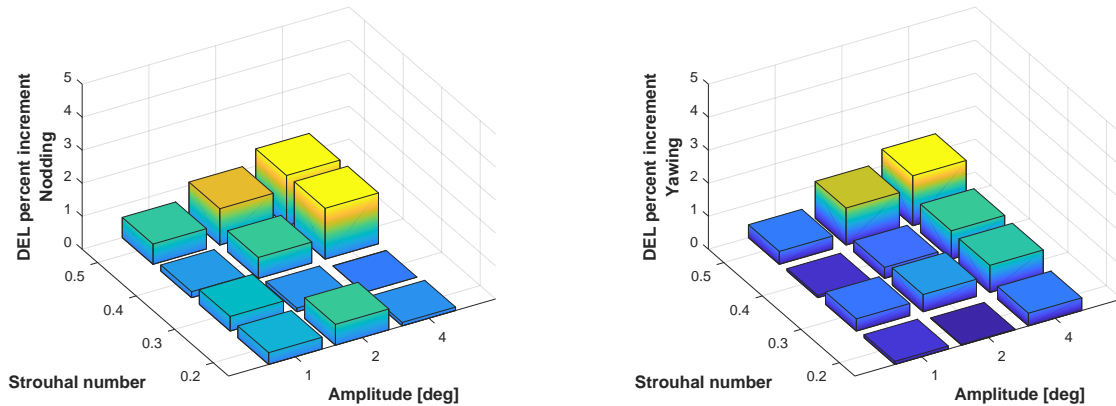


Figure 9. Weibull weighted DEL increases as function of amplitude and Strouhal number. Left: hub nodding moment. Right: hub yawing moment.

360 For this reason, in order to find the worst case, i.e. that condition which maximizes the increase of the load, 8 different 45-deg-spaced phases have been considered. Consequently, the full set of DLCs in Table 1 were simulated, for each couple of amplitude-Strouhal, eight times, by varying the phases φ_{PCM} .

Figure 10 shows the percentage increment for different combinations of Strouhal number and amplitude for blade root combined moment (up left) and tower base combined moment (up right) and hub combined moment (bottom). Above each bar, a text indicates the DLC which has generated that maximum load. Significant increases are only associated to blade loads, whereas hub and tower result to be not affected by PCM.

365

A sensitivity analysis was also conducted so as to compute the variation of maximum blade tip displacement. An increase up to 12% is measured for $\beta_{PCM} = 4$ deg, as shown in Fig. 11. This indication is extremely important as the maximum tip deflection typically enters as an active constraint into the design of the blade, affecting the thickness of its structural elements. If one excludes the highest PCM amplitude (i.e. 4 deg), the maximum tip deflection increases only of 3% which may correspond to a lower impact on blade design.

370

4.3 Comparison between periodic collective motion and wake redirection for the 10 MW INNWIND.EU turbine

Table 2 shows a comparison between the worst cases of WR control and PCM for the 10 MW INNWIND.EU turbine.

At first sight, PCM control with amplitude of 4 deg appears to be extremely impacting in terms of both fatigue and ultimate loads, with an increase of more than 10% in the maximum tip deflection which could be considered excessive, at least for the present machine whose design is constrained by this value. Excluding the previous case, the impact in terms of fatigue appears limited for both control techniques, especially if one considers the assumption that the wind farm control is always active no matter of the wind direction and TI. As noted in Zalkind and Pao (2016), in realistic farms, the amount of time spent with non-null inputs coming from the farm control layer can be rather small, yielding an even lower impact on fatigue.

375

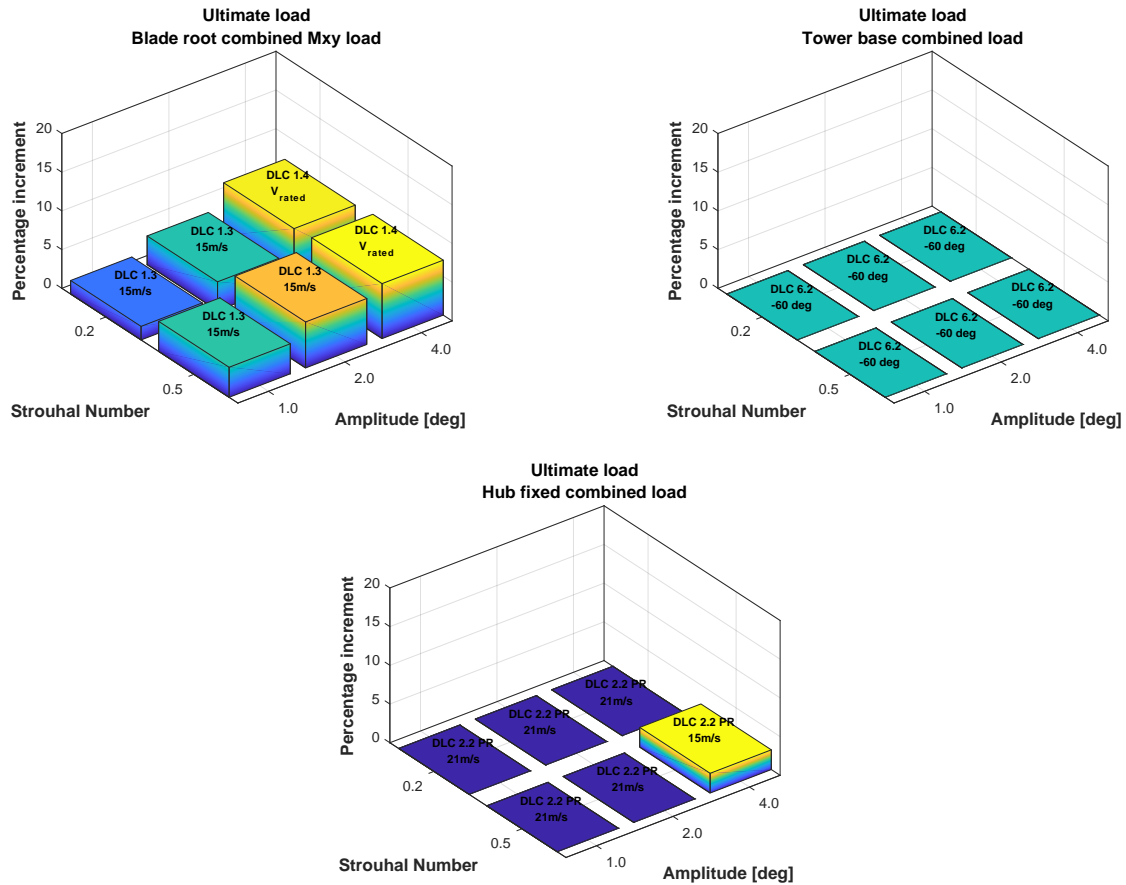


Figure 10. Maximum load increases as function of amplitude and Strouhal number. Up-left: blade root combined moment. Up-right: tower base combined moment. Bottom: hub combined moment.

380 If one considers, on the other hand, only the PCM with amplitude of 2 deg, the impact of PCM and WR becomes comparable, even though the latter seems less impacting especially for fatigue. In terms of ultimate loads, PCM has a higher impact on blade loads and null on tower, while the opposite happens for blade redirection.

Maximum tip deflection needs a special attention as both control techniques entail a significant increase in this quantity. In fact, for a typical glass-fiber blade, the blade-to-tower clearance is often an active constraint of the structural design (Sartori, 385 2019; Bortolotti et al., 2019). Moreover, in this case the load case resulting in the ultimate displacement is DLC 1.4 referring to an ECD, that is a deterministic wind case. This suggests that an ECD may happen regardless of the turbulence intensity which justifies, at least for the present study, the initial choice of neglecting a dependency between the TI and the activation of the wind farm controller.

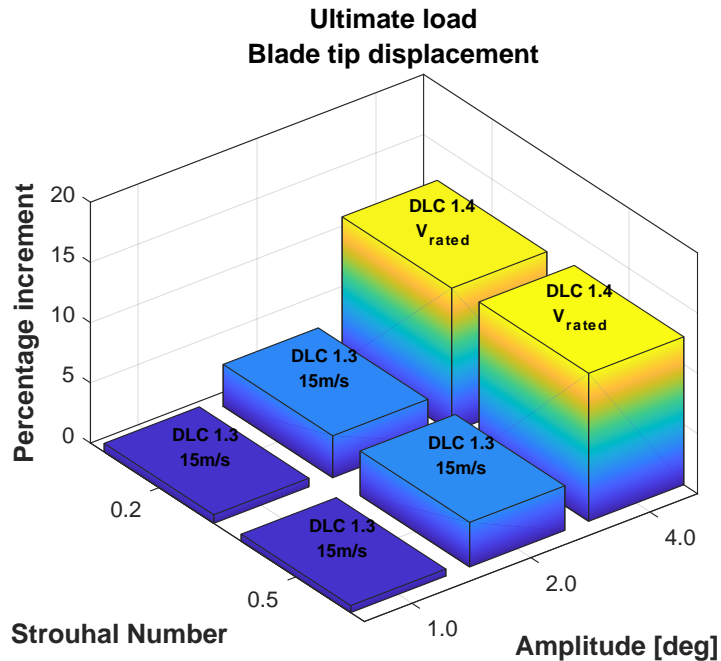


Figure 11. Blade tip maximum displacement increase as function of amplitude and Strouhal number.

Table 2. Comparison of worst cases (PCM vs WR)

	PCM		WR
	$A_{PCM} = 2 \text{ deg}$	$A_{PCM} = 4 \text{ deg}$	
AEP	-0.5 %	-2.2%	-18.4 % (at 30 deg)
ADC	+77 %	+143 %	-41 % (at 30 deg)
DEL blade flap	+7.2 %	+19.9 %	+3.5 % (at 30 deg)
DEL tower base fore-aft	+9.4 %	+32.9 %	+0.7 % (at 30 deg)
DEL hub	+1 %	+1 %	≈ 0 % (at 30 deg)
Ultimate blade root combined	+5.9 %	+7.1 %	+1.0 % (at 30 deg)
Ultimate tower base combined	0 %	0 %	+7.9 % (at 30 deg)
Ultimate hub combined	0 %	2.5 %	0 %
Max tip deflection	3 %	12.3 %	5.8 % (at 15 deg)

5 Evaluation of the impact of wind farm control on rotor design

390 In the Sec. 4, different wind farm control strategies have been analyzed with the aim of computing the related effect on wind turbine fatigue and ultimate loads, as well as on other important design parameters, such as the maximum blade deflection and

actuator duty cycles. The performed analyses showed that WR and PCM have a limited, but not negligible, effect on fatigue and, more important, a significant impact on ultimate loads, especially on the maximum tip deflection, which is a typical design driver for blades (i.e. a maximum blade tip displacement is severely enforced in the design process in order to maintain a suitable clearance between blades and tower).

This Section deals with the impact of wind farm control within the design of the turbine rotor, and can be considered as the subsequent step with respect to the study of Sec. 4.

The goal of this analysis is to quantify the possible modifications on the structural design of the blade if wind farm control is considered. Possible increase in blade mass and turbine cost will be considered as concise indicators of the impact of wind farm control on blade design.

Since the focus of this study is on the macroscopic impact of wind farm controllers on the design rather than to provide a fully-feasible structural layout, we limited our analysis to the aero-elastic optimization loop of Fig 2.

In order to perform a neat comparison where the effects of the sole wind farm control are highlighted, all redesigned rotors should be "optimal", in the sense that they should be all coming from an equal optimal design process characterized by the very same cost function and constraints, otherwise, it would be impossible to split the effects of the wind farm controller from those of the specific optimization strategy in the final comparison. To this end, the reference INNWIND.EU 10 MW wind turbine is firstly redesigned with C_{p-Max} following the procedure described in Sec. 3, yielding the "baseline" rotor. Then, the baseline configuration will be updated by the same optimization process but including this time the presence of the wind farm control. The considered wind farm control is the PCM characterized by $S_t = 0.5$ and $\beta_{PCM} = 2$ deg, while in Sartori et al. (2020) is reported a rotor design comparison which includes also the WR control.

The design process of the baseline generated an optimal solution compliant to all optimization constraints, with a structure mildly different with respect to the nominal INNWIND.EU. Hence, for the sake of brevity, the related detailed analysis is not reported in this manuscript.

5.1 Structural redesign with PCM

The structural optimization was then repeated by taking into account both the standard DLCs set from Table 1 and all the DLCs in which the turbine is controlled with the PCM. Different phase angles of the PCM were included in the ultimate loads/displacements analysis. Once again, the entire set of DLCs was re-computed at each structural iteration to make sure that, as the structural design evolves, the loads are updated accordingly.

The main results of the redesigned rotor with the PCM are summarized in Table 3. As shown, the introduction of the wind farm controller leads to a general deterioration of all key performance indicators. It must be stressed, however, that all indicators refer to the individual turbine as the current release of C_{p-Max} implements a turbine-specific cost model and a proper assessment of the impact of the PCM on the cost of energy should be evaluated at wind farm-level.

Concerning the aerodynamic performance, Table 3 shows that only a slight deterioration of the AEP is expected when the PCM is used. This is mainly due to the collective pitch motion imposed in the partial-loading range of the power curve,

Table 3. Comparison between the KPIs of the Baseline 10 MW and the redesigned rotor.

Performance	Baseline 10 MW	Redesign PCM	Variation
Blade mass:	40643 kg	45436 kg	+11.8%
AEP:	45.86 GWh	45.63 GWh	-0.5%
CoE:	89.42 EUR/MWh	90.22 EUR/MWh	+0.89%

which results in the collective pitch of the blades being cyclically driven away from their theoretical optimum value. This is confirmed by looking at the time-averaged turbulent power curve given in Fig. 12 (left) and the corresponding power coefficient (right). However, this detrimental influence is partially compensated by the increased stiffness of the blades which contribute to preserve the AEP by reducing the deformations experienced by the rotor. Another important feature of the PCM is the increase of Actuator Duty Cycle (see Fig. 13 (left)), which is a direct consequence of the increased service time required to the pitch actuators.

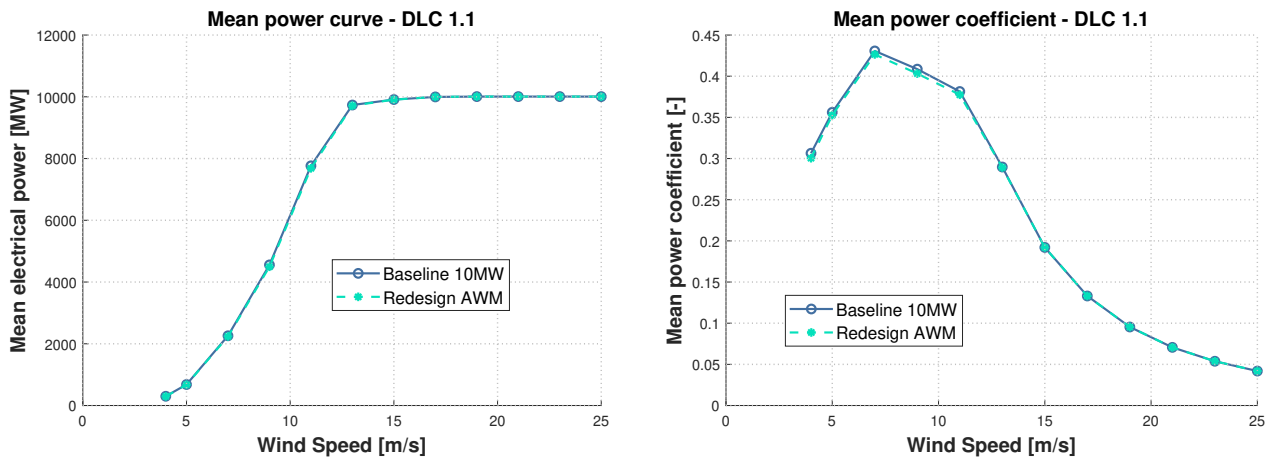


Figure 12. Redesign process including PCM. Left plot: time-averaged turbulent power curve. Right plot: power coefficient.

From a structural perspective, as expected, the introduction of the PCM resulted in an about 12% higher blade mass. This result comes from a combination of higher loads and higher displacements introduced by the wind farm controller. Specifically, the increased blade deflection required a heavy redesign of the spar caps in order to avoid the violation of the constraint on the maximum tip displacement. The optimal distribution of spar cap thickness is shown for both the baseline and the redesigned rotor in Fig. 14. It is worth to mention that, due to the increased flapwise stiffness, at the end of the optimization, the maximum displacement of the redesigned rotor is almost identical to that of the Baseline and, most importantly, it does not exceed the allowed tower clearance (see Fig. 13 (right)).

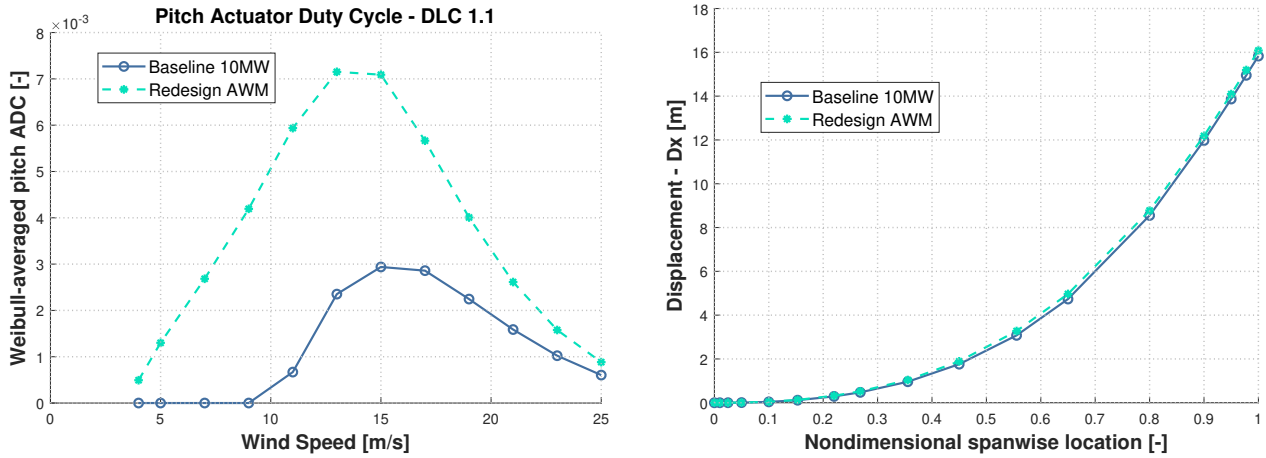


Figure 13. Redesign process including PCM. Left plot: Weibull-averaged ADC. Right plot: ultimate blade deflection.

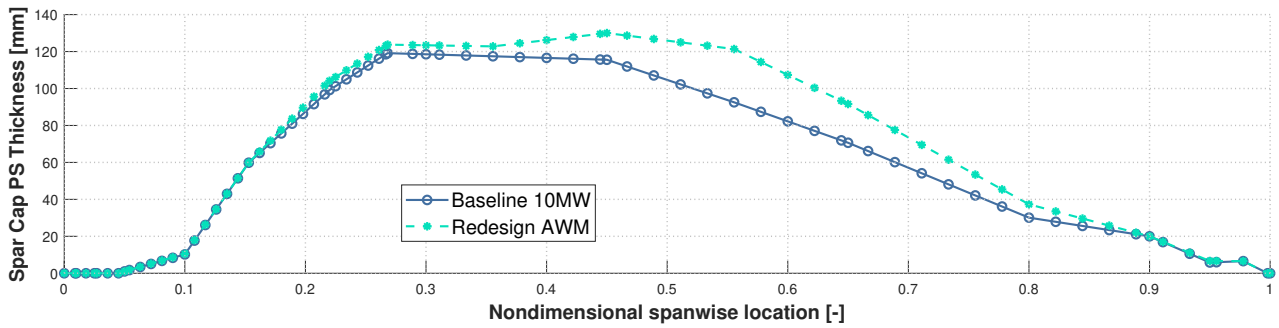


Figure 14. Redesign process including PCM: thickness distribution of the spar caps.

The fatigue DEL show a general increase of the loading in the rotor, although the impact on the the other sub-components, such as hub and tower, is less significant. This required a slight redesign of both the shell and the shear webs, as both elements are heavily driven by fatigue. This can be seen in the corresponding distributions of thickness provided by Fig. 15 and Fig. 16.

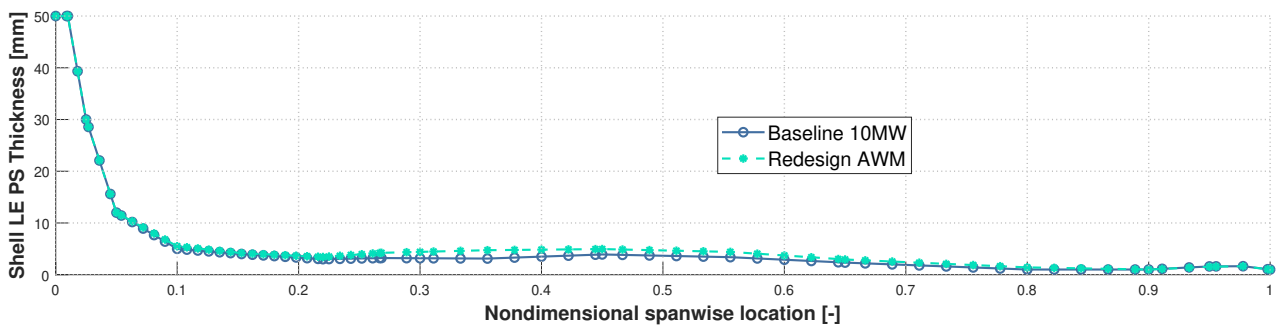


Figure 15. Redesign process including PCM: thickness distribution of the shell.

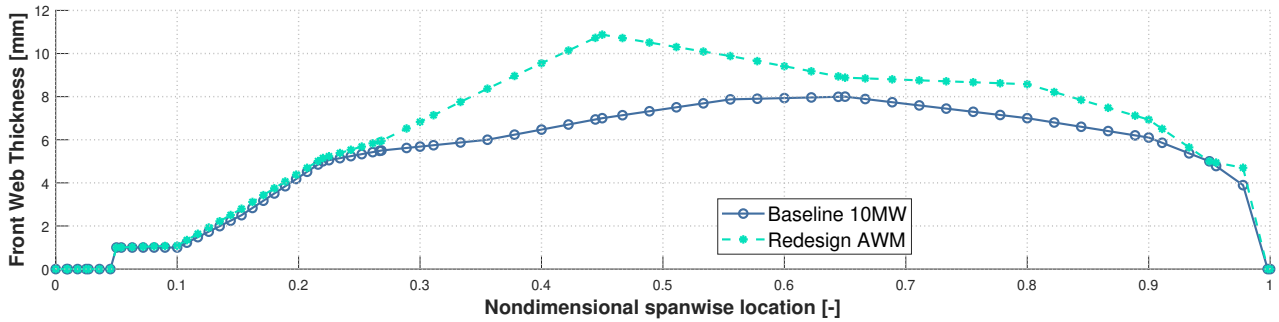


Figure 16. Redesign process including PCM: thickness distribution of the shear webs.

It must be also noticed that part of the fatigue increase is directly ascribable to the use of the PCM controller, but an important contribution is due to the increased blade mass. Then, an important conclusion is that fatigue loading should expect to increase not only for the use of the **wind farm** controller, but also due to the unavoidable mass increase required by the higher ultimate loads and displacements.

A complete comparison of the fatigue loads of the Redesign PCM rotor against the Baseline 10MW is given in Fig. 17, in which equivalent loads are made non-dimensional with the corresponding values of the Baseline 10MW. Here, f_{lp} identifies flapwise, edg is edgewise, trs is torsion, thr is thrust, nod is nodding, yaw is yawing, FA and SS are, respectively, fore-aft and side-side loads. As already discussed, the largest impact of the redesign in terms of fatigue is detected in the blade loads, in the hub thrust and, slightly, at the tower base fore-aft. The increase at tower base, however, would hardly justify a complete redesign of the tower.

The evolution of the ultimate loads follows a similar trend, with the worst effect being detected on the rotor. A direct comparison of the ultimate loading of the Baseline 10 MW and the Redesigned PCM is given in Fig. 17 (right). The nomenclature is similar to that of the fatigue analysis, however, here the tag cmb identifies multi-directional combined loads. From the diagram it is possible to notice how the blade loads are globally increased by the combination of PCM and higher blade mass. When it comes to the other sub-components, however, the impact is mixed. On one side, the side-side and the torsion at the tower base are slightly increased, while the fore-aft is significantly reduced. Based on this limited analysis, then, it is possible to conclude that the introduction of the PCM as a **wind farm** controller would require a redesign of the rotor but, likely, would not affect the structural integrity of the hub and the tower.

460 6 Conclusion and Outlook

In this paper, a procedure to evaluate the effects of wind farm control techniques on a single wind turbine has been developed. Two different control methods (dynamic induction control and the wake redirection) have been considered and tested on a reference 10 MW wind turbine. The study is **conducted** by simulating a wind turbine equipped with the chosen **wind farm control** according to the load cases prescribed by Standards, in order to identify the worst case scenario in terms of design

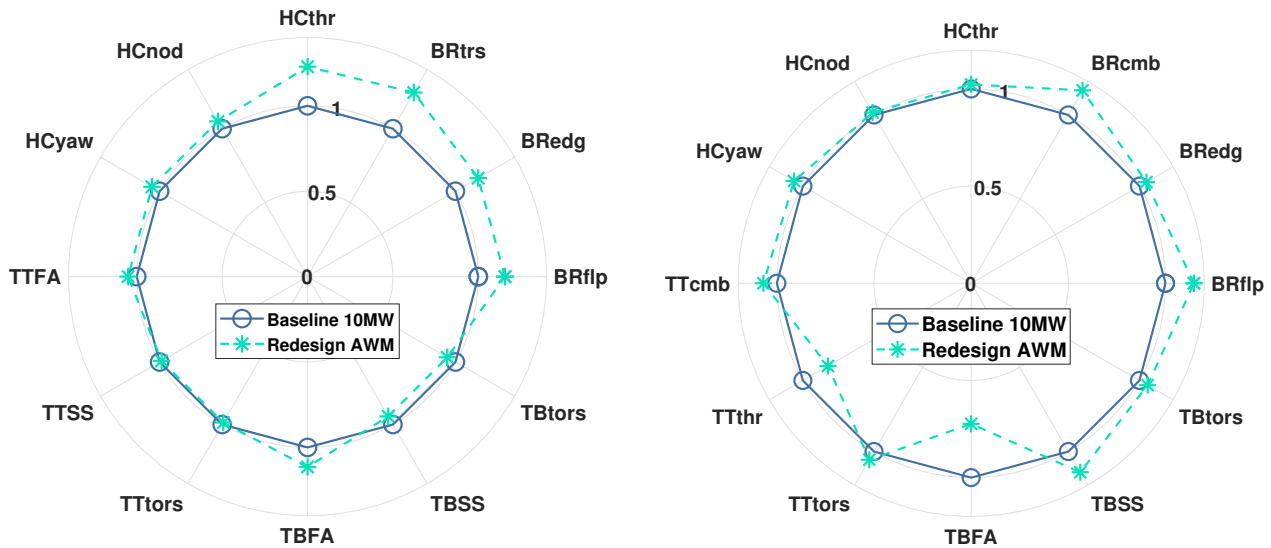


Figure 17. Comparison between PCM-redesigned and Baseline 10MW turbine. Left plot: fatigue DEL. Right plot: ultimate loads. ‘BR’ is blade root, ‘HC’ is hub center, ‘TT’ is tower top and TB is tower base

465 loads. In this strategy, an explicit dependency of the **wind farm control** on the turbulence intensity was neglected, whereas the value of turbulence intensity was always defined according to the turbine’s class. Although this limits the validity of the conclusions to the turbine under investigation, it allows to obtain results which are compatible with current Standards, and **which** are not site-specific. The findings of this study, however, suggest that **an extension** of the Standards in order to directly account for certain **wind farm controls** is recommendable.

470 The study has been performed through two steps. At first, the impact of the controls is evaluated in terms of the turbine KPI. The study has been conducted as a sensitivity analysis where all indicators are computed as functions of the **wind farm control** parameters. At this step, we were able to quantify the impact of the **controls** on the performance of an existing turbine and to define the operational limits of the wind farm controller to not exceed the original load spectra. In a second step, a dedicated structural redesign of the rotor has been performed in order to quantify how much the design would **have changed** if a **wind**
 475 **farm control had been** considered from the beginning.

From the analyses performed in this work the following conclusions can be derived:

- The impact of both controls in terms of fatigue is significant but does not seem particularly dramatic, especially if one considers that the wind farm control could be active for a limited range of wind directions, i.e. for only those directions for which a wake impingement is detected on downstream rotor.
- 480 – In some cases, the wake redirection control entails a reduction of the fatigue. The reason for this is to be found in the fact that operating in yawed conditions reduces the normal component of the wind with respect to the rotor disk, lowering loads.

- 485
- The most impacting control seems to be the one based on the dynamic induction, especially if higher amplitudes of the blade pitch angles are considered. However, if the amplitude is maintained below 2 deg, the potential increase in fatigue is limited.
 - Tower ultimate loads are particularly affected by wake redirection, with the ECD condition being the most impacting DLC.
 - The blade loads, on the other hand, are mostly affected by dynamic induction control.
 - Both controls lead to an increase in the maximum tip displacements. Since the turbine considered in this study is heavily constrained by tip deflection, this results in a significant mass increase when the rotor is redesigned. It must be noticed that different design concepts (or materials) could result in different sizing loads and, therefore, to different impacts on the redesign.
 - The redesign process led to an increased rotor mass: due to the heavier blades, most fatigue loads along the turbine increase accordingly. Then, in this study, the main impact on the fatigue loads is actually the mass increase, whilst the impact directly correlated to the adoption of the **wind farm control** is neglectable.
- 490
- 495

It is important to stress that these findings only apply to the considered wind turbine, and may be different for other machines. Future developments of this work will try to investigate this aspect by considering different turbine classes, design concepts and materials. In addition, it would also be interesting to include the redesign of the tower internal structure in a more specific investigation. **Connected to tower design, it could be also interesting to consider a different dynamic induction control strategy based on individual pitch control, which entails a lower variation of thrust and which could have in turn a milder impact on blade loading (Frederik et al., 2020a).**

500

In terms of extensions of the present research, the evaluation of the impact of farm control on ultimate and fatigue loads of downstream turbines is certainly an interesting topic, which deserves dedicated analyses with more sophisticated tools than those used in the present work to simulate the wind farm flow, e.g. CFD or dynamic wake models (Cacciola et al., 2020b).

505 Another important direction for future **works** deals with the assessment of the economic impact of **wind farm control** at wind-farm level. To this end, specific studies will be done to consider not only the impact of the chosen **wind farm control** on the turbine loads but also the beneficial effects that the chosen **wind farm control** have on the wind farm power production and, possibly, on its cost of energy.

Author contributions. All authors provided fundamental input to this research work through discussions, feedback and analyses of the state of the art. PDF conducted the sensitivity analysis with the WR control, SC conducted the sensitivity analysis with the PCM, LS performed the structural design, AC developed the main idea behind this work and supervised the research activities. SC, AC and LS wrote the manuscript.

510

Competing interests. No competing interests are present

Acknowledgements. This work has been partially supported by the CL-Windcon project, which receives funding from the European Union Horizon 2020 research and innovation program under grant agreement No. 727477.

515 References

- Annoni, J., Gebraad, P. M., Scholbrock, A. K., Fleming, P., and v. Wingerden, J.-W.: Analysis of axial-induction-based wind plant control using an engineering and a high-order wind plant model., *Wind Energy*, 19, 1135–1150, 2016.
- Bauchau, O. A.: Flexible Multibody Dynamics, vol. 176 of *Solid Mechanics and Its Applications*, Springer Netherlands, 1 edn., 2011.
- Boorsma, K.: Power and loads for wind turbines in yawed conditions — Analysis of field measurements and aerodynamic predictions, Tech. Rep. ECN-E-12-047, ECN – Energy research Center of the Netherlands, 2012.
- 520 Bortolotti, P., Bottasso, C. L., and Croce, A.: Combined preliminary–detailed design of wind turbines, *Wind Energy Science*, 1, 71–88, <https://doi.org/10.5194/wes-1-71-2016>, <https://www.wind-energ-sci.net/1/71/2016/>, 2016.
- Bortolotti, P., Bottasso, C. L., Croce, A., and Sartori, L.: Integration of multiple passive load mitigation technologies by automated design optimization—The case study of a medium-size onshore wind turbine, *Wind Energy*, 22, 65–79, <https://doi.org/10.1002/we.2270>, <https://onlinelibrary.wiley.com/doi/abs/10.1002/we.2270>, 2019.
- 525 Bossanyi, E.: Combining induction control and wake steering for wind farm energy and fatigue loads optimisation, *Journal of Physics: Conference Series*, 1037, 032 011, <https://doi.org/10.1088/1742-6596/1037/3/032011>, <https://doi.org/10.1088%2F1742-6596%2F1037%2F3%2F032011>, 2018.
- Bottasso, C. L. and Croce, A.: Cp-Lambda user manual, Tech. rep., Dipartimento di Scienze e Tecnologie Aerospaziali, Politecnico di Milano, 530 Milano, Italy, 2009–2018.
- Bottasso, C. L., Croce, A., Savini, B., Sirchi, W., and Trainelli, L.: Aero-servo-elastic modeling and control of wind turbines using finite element multibody procedures, *Multibody Systems Dynamics*, 16, 291–308, 2006.
- Cacciola, S., Bertozzi, A., Sartori, L., and Croce, A.: On the dynamic response of a pitch/torque controlled wind turbine in a pulsating dynamic wake, *Journal of Physics: Conference Series*, 1618, 062 033, <https://doi.org/10.1088/1742-6596/1618/6/062033>, 2020a.
- 535 Cacciola, S., Bertozzi, A., Sartori, L., and Croce, A.: On the dynamic response of a pitch/torque controlled wind turbine in a pulsating dynamic wake, *Journal of Physics: Conference Series*, 1618, 062 033, <https://doi.org/10.1088/1742-6596/1618/6/062033>, <https://doi.org/10.1088%2F1742-6596%2F1618%2F6%2F062033>, 2020b.
- Cardaun, M., Roscher, B., Schelenz, R., and Jacobs, G.: Analysis of Wind-Turbine Main Bearing Loads Due to Constant Yaw Misalignments over a 20 Years Timespan, *Energies*, 12, <https://doi.org/10.3390/en12091768>, <https://www.mdpi.com/1996-1073/12/9/1768>, 2019.
- 540 CL-Windcon: Closed Loop Wind Farm Control, <http://www.clwindcon.eu/>, european Union Horizon 2020 research and innovation program, grand agreement No. 727477, 2016 -2019.
- Damiani, R., Dana, S., Annoni, J., Fleming, P., Roadman, J., van Dam, J., and Dykes, K.: Assessment of wind turbine component loads under yaw-offset conditions, *Wind Energy Science*, 3, 173–189, <https://doi.org/10.5194/wes-3-173-2018>, <https://www.wind-energ-sci.net/3/173/2018/>, 2018.
- 545 DTU: The DTU 10MW Reference Wind Turbine Project Site, <http://dtu-10mw-rwt.vindenergi.dtu.dk/>, 2012.
- Ennis, B. L., White, J. R., and Paquette, J. A.: Wind turbine blade load characterization under yaw offset at the SWiFT facility, *Journal of Physics: Conference Series*, 1037, 052 001, <https://doi.org/10.1088/1742-6596/1037/5/052001>, <https://doi.org/10.1088%2F1742-6596%2F1037%2F5%2F052001>, 2018.
- 550 Fingersh, L., Hand, M., and Laxson, A.: Wind Turbine Design Cost and Scaling Model, Tech. Rep. NREL/TP-500-40566, National Renewable Energy Laboratory, 2006.

- Fleming, P., King, J., Dykes, K., Simley, E., Roadman, J., Scholbrock, A., Murphy, P., Lundquist, J. K., Moriarty, P., Fleming, K., van Dam, J., Bay, C., Mudafort, R., Lopez, H., Skopek, J., Scott, M., Ryan, B., Guernsey, C., and Brake, D.: Initial results from a field campaign of wake steering applied at a commercial wind farm – Part 1, *Wind Energy Science*, 4, 273–285, <https://doi.org/10.5194/wes-4-273-2019>, <https://www.wind-energ-sci.net/4/273/2019/>, 2019.
- 555 Frederik, J. A., Doekemeijer, B. M., Mulders, S. P., and van Wingerden, J.-W.: The helix approach: Using dynamic individual pitch control to enhance wake mixing in wind farms, *Wind Energy*, 23, 1739–1751, <https://doi.org/https://doi.org/10.1002/we.2513>, <https://onlinelibrary.wiley.com/doi/abs/10.1002/we.2513>, 2020a.
- Frederik, J. A., Weber, R., Cacciola, S., Campagnolo, F., Croce, A., Bottasso, C., and van Wingerden, J.-W.: Periodic dynamic induction control of wind farms: proving the potential in simulations and wind tunnel experiments, *Wind Energy Science*, 5, 245–257, <https://doi.org/10.5194/wes-5-245-2020>, <https://www.wind-energ-sci.net/5/245/2020/>, 2020b.
- 560 Gebraad, P., Thomas, J. J., Ning, A., Fleming, P., and Dykes, K.: Maximization of the annual energy production of wind power plants by optimization of layout and yaw-based wake control, *Wind Energy*, 20, 97—107, 2017.
- Gebraad, P. M. O., Teeuwisse, F. W., van Wingerden, J. W., Fleming, P. A., Ruben, S. D., Marden, J. R., and Pao, L. Y.: Wind plant power optimization through yaw control using a parametric model for wake effects—a CFD simulation study, *Wind Energy*, 19, 95–114, <https://doi.org/10.1002/we.1822>, <https://onlinelibrary.wiley.com/doi/abs/10.1002/we.1822>, 2016.
- 565 Kanev, S., Savenije, F., and Engels, W.: Active wake control: An approach to optimize the lifetime operation of wind farms, *Wind Energy*, 21, 488–501, <https://doi.org/10.1002/we.2173>, <https://onlinelibrary.wiley.com/doi/abs/10.1002/we.2173>, 2018.
- Knudsen, T., Bak, T., and Svenstrup, M.: Survey of wind farm control—power and fatigue optimization, *Wind Energy*, 18, 1333–1351, <https://doi.org/10.1002/we.1760>, <https://onlinelibrary.wiley.com/doi/abs/10.1002/we.1760>, 2015.
- 570 IEC 61400-1 Ed.3.: Wind Turbines — Part 1: Design requirements, Tech. rep., Garrad Hassan and Partners Ltd, St Vincent’s Works, Silverthorne Lane - Bristol BS2 0QD, UK, 2004.
- IK4 Research Alliance: IK4 Baseline controller for INNWIND 10MW wind turbine, <https://github.com/ielorza/OpenDiscon>, 2016.
- Mendez Reyes, H., Kanev, S., Doekemeijer, B., and van Wingerden, J.-W.: Validation of a lookup-table approach to modeling turbine fatigue loads in wind farms under active wake control, *Wind Energy Science*, 4, 549–561, <https://doi.org/10.5194/wes-4-549-2019>, <https://www.wind-energ-sci.net/4/549/2019/>, 2019.
- 575 Munters, W. and Meyers, G.: An optimal control framework for dynamic induction control of wind farms and their interaction with the atmospheric boundary layer., *Philosophical Transactions of the Royal Society A: Mathematical, Physical and Engineering Sciences*, 375, 20160 100–1–19, 2017.
- Munters, W. and Meyers, G.: Towards practical dynamic induction control of wind farms: analysis of optimally controlled wind-farm boundary layers and sinusoidal induction control of first-row turbines., *Wind Energy Science*, 3, 409—425, 2018.
- 580 NREL: FLORIS. Version 1.0.0, <https://github.com/NREL/floris>, 2019.
- Riboldi, C. E. D.: Advanced control laws for variable-speed wind turbines and supporting enabling technologies, Ph.D. thesis, Politecnico di Milano, 2012.
- Sartori, L.: System design of lightweight wind turbine rotors, Ph.D. thesis, Politecnico di Milano, https://www.politesi.polimi.it/bitstream/10589/144667/3/2019_01_PhD_Sartori_b.pdf, 2019.
- 585 Sartori, L., De Fidelibus, P., Cacciola, S., and Croce, A.: Wind turbine rotor design under wind farm control laws, *Journal of Physics: Conference Series*, 1618, 042 027, <https://doi.org/10.1088/1742-6596/1618/4/042027>, 2020.

- Urbán, A. M., Larsen, T. J., Larsen, G. C., Held, D. P., Dellwik, E., and Verelst, D.: Optimal yaw strategy for optimized power and load in various wake situations, *Journal of Physics: Conference Series*, 1102, 012019, <https://doi.org/10.1088/1742-6596/1102/1/012019>, <https://doi.org/10.1088/1742-6596/1102/1/012019>, 2018.
- 590
- White, J., Brandon, E., and Herges, T. G.: Estimation of Rotor Loads Due to Wake Steering, in: *Wind Energy Symposium 2018*, Kissimmee, Florida, <https://doi.org/10.2514/6.2018-1730>, <https://arc.aiaa.org/doi/abs/10.2514/6.2018-1730>, 2018.
- Zalkind, D. S. and Pao, L. Y.: The fatigue loading effects of yaw control for wind plants, in: *2016 American Control Conference (ACC)*, pp. 537–542, 2016.
- 595
- Ziegler, L., Gonzalez, E., Rubert, T., Smolka, U., and Melero, J. J.: Lifetime extension of onshore wind turbines: A review covering Germany, Spain, Denmark, and the UK, *Renewable and Sustainable Energy Reviews*, 82, 1261 – 1271, <https://doi.org/https://doi.org/10.1016/j.rser.2017.09.100>, <http://www.sciencedirect.com/science/article/pii/S1364032117313503>, 2018.